A sucrose-utilisation gene cluster contributes to colonisation of horse chestnut by Pseudomonas syringae pv. aesculi

Molecular Plant Pathology

WILEY

Molecular Plant Pathology

ORIGINAL ARTICLE OPEN ACCESS

A Sucrose-Utilisation Gene Cluster Contributes to Colonisation of Horse Chestnut by *Pseudomonas syringae* pv. *aesculi*

Sabrine Dhaouadi[1] | Diana Vinchira-Villarraga[1] | Sanju Bijarniya[1] | Amy J. Webster[1] | Federico Dorati[2] | Carrie Brady[3] | Dawn L. Arnold[4] | Mojgan Rabiey[1,5] | Robert W. Jackson[1]

[1]School of Biosciences and the Birmingham Institute of Forest Research, University of Birmingham, Birmingham, UK | [2]School of Biosciences, University of Reading, Reading, UK | [3]School of Applied Sciences, College of Health, Science and Society, University of the West of England, Bristol, UK | [4]Harper Adams University, Newport, UK | [5]School of Life Sciences, Gibbet Hill Campus, University of Warwick, Coventry, UK

Correspondence: Sabrine Dhaouadi (s.dhaouadi@bham.ac.uk)

Received: 18 February 2025 | **Revised:** 1 May 2025 | **Accepted:** 9 June 2025

Funding: This work was supported by JAABS private foundation.

Keywords: mutagenesis | pathogen–host interactions | *Pseudomonas syringae* | sucrose metabolism | type III secretion system (T3SS) | virulence factors

ABSTRACT

Pseudomonas syringae pathovar *aesculi* (E-*Pae*) causes bleeding canker disease in the woody tissue of European horse chestnut (HC). Comparative genomic analysis of E-*Pae* with a related leaf-infecting strain (I-*Pae*) and other *P. syringae* strains identified candidate virulence genes for colonisation of woody tissue, including a sucrose uptake and utilisation system (*scrYABCDBR* cluster) found in 162 of 206 *P. syringae* strains spanning the pangenome. Growth analysis using sucrose as sole carbon source showed that I-*Pae* (lacking the gene cluster) was unable to grow whereas E-*Pae* could grow. *P. savastanoi* pv. *phaseolicola* 1448A and *P. syringae* pv. *morsprunorum* R15244 were compromised in growth despite the presence of the gene cluster. Sucrose utilisation assays using *scrB* and *scrY* mutants and complemented strains confirmed the importance of the cluster for sucrose metabolism in vitro. Pathogenicity assays in HC revealed the sucrose gene cluster is important for symptom development in the woody tissue. While the *scr* genes contribute to disease causation, they were not essential for pathogen fitness when compared to *hrpL* and *hopAB1* mutants. E-*Pae* caused disease symptoms in HC leaves, suggesting the strain has the potential to infect leaves as well. However, it was notable that the *scrB* mutant of E-*Pae* caused increased disease symptoms, possibly highlighting a niche adaptation strategy for I-*Pae* to cause leaf spots in HC as well as constraining E-*Pae* to predominantly infect the woody tissue.

1 | Introduction

The bleeding canker disease of European horse chestnut (*Aesculus hippocastanum*) (HC) is widespread in Europe, including the British Isles, following a recent epidemic that has caused severe damage and death to thousands of HC trees (Green et al. 2009; Dijkshoorn-Dekker and Kuik 2005; Green et al. 2010; Mertelik et al. 2013; Schmidt et al. 2008; Webber et al. 2008; Bultreys et al. 2008).

The disease symptoms include dark lesions or cankers on the trunk or branches of the tree that exude a dark, reddish-brown fluid. Severe infections can lead to dieback of branches, leaf discolouration and eventually, the death of the tree if the canker girdles the stem (de Keijzer et al. 2012; Green et al. 2009; Steele et al. 2010; Webber et al. 2008). These symptoms are caused by the European (E) genotype of *Pseudomonas syringae* pathovar *aesculi* (E-*Pae*) that is related to an isolate causing leaf spots in Indian HC (*Aesculus indica*) (I-*Pae*) (Durgapal

and Singh 1980). E-*Pae* causes severe symptoms and thus represents a major disease for HC. Analysis of cankers on the main stem, branches and young shoots showed that lesions form in the cortex and phloem and extend into the cambium (de Keijzer et al. 2012; Green et al. 2009; Steele et al. 2010), thus can severely impact water and nutrient transport and kill the tree.

Phylogenomic analysis revealed that Pae genomes (E-*Pae* and I-*Pae*) share the greatest sequence similarity with *P. syringae* strains from herbaceous hosts, such as *P. syringae* pv. *phaseolicola* 1448A (*Pph* 1448A) and *P. syringae* pv. *tabaci* (*Pta* 11528) infecting bean and tobacco, respectively (Green et al. 2010). Pae (E-*Pae* and I-*Pae*) is also phylogenomically related with pathovars that colonise woody hosts, such as *P. syringae* pathovars *cerasicola*, *savastanoi*, *morsprunorum* race 1 and *P. amygdali*, which infect ornamental cherry, olive, sweet and sour cherries and almond, respectively (Ruinelli et al. 2019). However, 15% of the *Pae* genome is uniquely conserved, which may contribute to its adaptation to woody hosts. This suggests an evolutionary relationship where *Pae* has diverged from other pathovars to colonise and infect HC.

It has been hypothesised that some of the genomic regions conserved in *Pae* genomes are likely responsible for their association with a tree host (Green et al. 2010; Nowell et al. 2016). Moreover, there are unique genetic regions in both E-*Pae* and I-*Pae* likely indicating intimate host adaptations to enable bacterial colonisation in the tree's wood or leaf tissues (Green et al. 2010; Nowell et al. 2016). For example, there are differences in the collection of type III secretion system (T3SS) effectors (T3SE) between E-*Pae* and I-*Pae* as well as genes related to urea metabolism, β-ketoadipate and protocatechuate-4,5-deoxygenase pathways, degradation of aromatic compounds, fatty acid biosynthesis and degradation, sucrose utilisation and iron uptake (Green et al. 2010; Nowell et al. 2016). Some of these could explain the adaptation of E-*Pae* to the woody tissue niche, distinguishing it from the leaf coloniser I-*Pae*.

The putative sucrose uptake and utilisation gene cluster present in E-*Pae* (but not I-*Pae*) is formed of seven genes (*scrYABCDBR*) including a putative porin (*scrY*) likely involved in the transport of sucrose into the cell (Hardesty et al. 1991; Reid and Abratt 2005; Sun et al. 2016) and a sucrose invertase enzyme (*scrB*) probably involved in the enzymatic digestion of sucrose to glucose and fructose (Engels et al. 2008; Gunasekaran et al. 1990; Reid et al. 1999; Reid and Abratt 2005). In the plant, sucrose is produced by photosynthesis and distributed throughout the plant, thus having an uptake and digestion system would likely enhance the fitness of the pathogen (Braun et al. 2013; Tauzin and Giardina 2014). We hypothesised that E-*Pae*'s ability to access and utilise sucrose enhances its capacity to efficiently colonise the phloem of stems and branches unlike I-*Pae*, which lacks the necessary genetic machinery for sucrose metabolism.

2 | Results

2.1 | Genetic Analysis of a Putative Sucrose Gene Cluster in E-*Pae* 2250 and Other *P. syringae* Strains

E-*Pae* 2250 possesses an 8.6 kb gene cluster on the chromosome containing seven genes predicted to be involved with sucrose uptake and utilisation (see Table 1 for coordinates and Figure 1A for gene orientation). A pangenome analysis using 206 *P. syringae* and other *Pseudomonas* strains, spanning 13 phylogroups, representing 16 species and 37 pathovars, was conducted to determine if the gene cluster is widespread (Table S1). Of the 206 strains analysed, 162 (79%) carried the *scr* gene cluster, while 44 (21%) did not (Figure 1C). Among the 80 strains isolated from woody hosts, all carried the *scr* cluster, suggesting strong conservation of this operon in woody plant-associated strains. In contrast, among strains from non-woody hosts ($n = 100$), only 82 possessed the cluster, while the remaining 18 lacked it. The 25 strains with unknown host information showed a mixed distribution (Table S1,S6). The cluster was found in strains isolated from leaves ($n = 88$) and wood ($n = 57$), with presence generally correlating with strains infecting perennial hosts.

TABLE 1 | Sucrose-utilisation-associated genes found in the annotated genome of *Pseudomonas syringae* pv. *aesculi* strain 2250.

Gene name	CDS	Locus tag	Start	End	Gene product	Protein ID
Gene 1 (*scrY*)	5939523...5941100	QFG70_26900	5939523	5941100	Carbohydrate porin	WGQ00723.1
Gene 2	5941268...5942542	QFG70_26905	5941268	5942542	ABC transporter substrate-binding protein	WGQ00724.1
Gene 3	5942564...5943526	QFG70_26910	5942564	5943526	Sugar ABC transporter permease	WGQ00725.1
Gene 4	5943523...5944365	QFG70_26915	5943523	5944365	Carbohydrate ABC transporter permease	WGQ00726.1
Gene 5 (*ugpC*)	5944393...5945538	QFG70_26920	5944393	5945538	Sn-glycerol-3-phosphate ABC transporter ATP-binding protein UgpC	WGQ00727.1
Gene 6 (*scrB*)	5945535...5947049	QFG70_26925	5945535	5947049	Glycoside hydrolase family 32 protein	WGQ00728.1
Gene 7	5947117...5948109	QFG70_26930	5947117	5948109	LacI family DNA-binding transcriptional regulator	WGQ00729.1

2.2 | The *Scr* Gene Cluster Is Used by E-*Pae* 2250 to Utilise Sucrose

E-*Pae* strain 2250 was tested for growth in minimal medium containing sucrose (10 or 50 mM) as the sole carbon source. Two other strains carrying putative sucrose utilisation clusters were included: a cherry pathogen *P. syringae* pv. *morsprunorum* (*Psm*) R15244 and a bean pathogen *Pph* 1448A. Additionally, the Indian *Pae* strain (I-*Pae* 3681), which lacks the sucrose gene cluster, was included for comparison. All the *Pseudomonas* strains grew

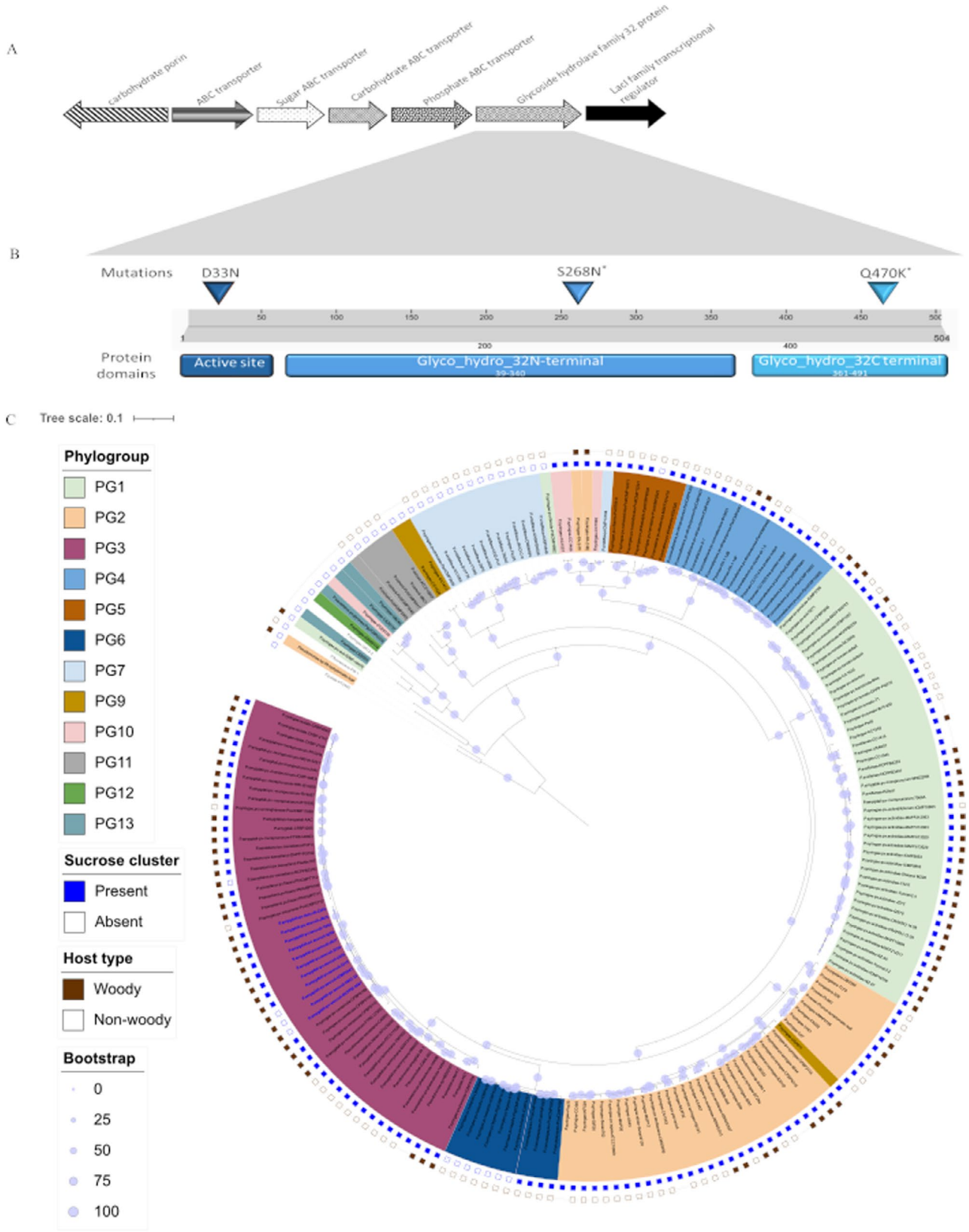

FIGURE 1 | Legend on next page.

FIGURE 1 | Comparative analysis of sucrose metabolism gene clusters across *Pseudomonas syringae* strains. (A) Genomic organisation of sucrose metabolism gene clusters in *Pseudomonas syringae* pv. *aesculi* (E-*Pae* 2250) with annotations for the specific genes and their functions including carbohydrate porin, ABC transporter substrate-binding protein, sugar ABC transporter permease, carbohydrate ABC transporter permease, phosphate ABC transporter ATP-binding protein, sucrose-6-phosphate hydrolase, LacI-family sucrose transcriptional regulator. (B) InterProScan visualisation of ScrB protein with its annotated functional domains and conserved residues, where residues 268 and 470 are located in the N-terminal and the C-terminal domains, respectively. (C) Phylogenetic tree of *Pseudomonas* phylogroups based on core genome alignment. The phylogenetic tree was generated from a pangenome analysis using Panaroo, focusing on core gene alignment. The maximum-likelihood phylogeny was constructed using IQ-TREE, employing the ModelFinder Plus (MFP) and AUTO commands to identify the best-fit substitution model and optimise CPU usage, respectively. Bootstrap support values were calculated with 1000 replicates to assess the robustness of the tree. The visualisation, produced with iTOL v. 6, highlights the distribution of *Pseudomonas* phylogroups (PG1 to PG13) with sucrose gene cluster presence (blue squares) or absence (white squares), along with bootstrap values shown by varying circle sizes. A strain without a square indicates the source of isolation is unknown.

well in Luria Bertani (LB) medium, and none showed any significant growth in M9 minimal medium lacking a carbon source (Figure S1). Only E-*Pae* 2250 demonstrated substantial growth in M9+ sucrose, reaching an OD_{600} of 0.35 and 0.6 after 24 h in 10 and 50 mM sucrose, respectively (Figure 2A,B). *Psm* R15244 showed only slight growth in 10 mM sucrose, but after displaying an initial lag phase, it reached an OD_{600} of 0.5 in 50 mM sucrose. In contrast, I-*Pae* 3681 and *Pph* 1448A displayed no measurable growth in either sucrose medium. These growth phenotype differentials were supported by two-way repeated measures ANOVA, which showed significant effects of strain, time and their interaction at both sucrose concentrations ($p < 0.001$; Figure S2A,B). Post hoc Tukey Kramer's tests revealed that E-*Pae* 2250 grew significantly better than all other strains at all timepoints (1000, 2000 and 3000 min) in 10 mM sucrose ($p < 0.001$). At 50 mM sucrose, E-*Pae* 2250 also outperformed all strains at 1000 and 2000 min ($p < 0.001$), although by 3000 min the difference with *Psm* R15244 was not statistically significant.

The different phenotypes of *Psm* R15244 and *Pph* 1448A in utilising sucrose suggested that differences in either the regulatory systems or the *scr* gene clusters in these strains were responsible for reducing the effectiveness of either uptake or breakdown of sucrose. Analysis of the nucleotide and protein sequences of the *scr* genes of E-*Pae* 2250, *Psm* R14255 and *Pph* 1448A revealed that the seven genes had conserved synteny and similar nucleotide (nt) sequence lengths of the genes (Table 2). However, several nt differences were observed in the seven genes (Table 2), with more variations observed in the *Pph* genes. The most conserved gene was the putative transcriptional regulator, with 100% identity in *Psm* R14255 and 99.70% identity in *Pph* 1448A (corresponding to five nt differences and one amino acid [aa] change). Larger variations were seen in the other six genes, whereby predicted proteins had 1–12 aa changes. The carbohydrate porin ScrY was different by 3 and 4 aa, and the invertase ScrB exhibited 3 and 12 aa differences, in *Psm* R14255 and *Pph* 1448A, respectively. Given the putative roles of carbohydrate porin (ScrY) in sucrose uptake and of the invertase enzyme (ScrB) in sucrose breakdown, we focused our analysis on these as representatives of the two processes.

2.3 | The Invertase Gene *scrB* and Carbohydrate Porin *scrY* Are Essential for E-*Pae* 2250 Sucrose Utilisation

To test the hypothesis that *scrB* and *scrY* genes are crucial for the sucrose growth phenotype displayed by E-*Pae*, we constructed insertional knockout mutants for *scrB* (E-*Pae* 2250::*scrB*) and *scrY* (E-*Pae* 2250::*scrY*) and created complemented strains using cloned full-length *scrB* and *scrY* genes. Growth assays with M9 + 50 mM sucrose demonstrated that inactivation of both *scrB* and *scrY* significantly reduced the ability of E-*Pae* 2250 to grow, with the *scrB* inactivation having a bigger impact on E-*Pae* growth (Figure 2C,D). The complemented strains restored growth comparable to the wild-type (WT) E-*Pae* 2250 strain. The doubling times of the WT, E-*Pae* 2250::*scrB*, E-*Pae* 2250::*scrY*, complemented strains and empty vector controls, in M9 + 50 mM sucrose (data not shown) showed subtly different phenotypes for the mutants (WT 1639 min vs. E-*Pae* 2250::*scrB* 2231 min and E-*Pae* 2250::*scrY* 1732 min). Complementation of E-*Pae* 2250::*scrB* with *scrB* increased doubling time to 1639 min, while complementation of E-*Pae* 2250::*scrY* with *scrY* substantially improved doubling time to even better than the WT (1377 min). These phenotype differentials were supported by statistical analysis (Figure S2C,D), where two-way repeated measures ANOVA showed significant effects of strain, time and their interaction ($p < 0.001$). Post hoc Tukey–Kramer's tests confirmed that the *scrB* mutant exhibited significantly reduced growth at 1000 and 2000 min ($p < 0.001$), while the *scrY* mutant was significantly different only at 2000 min ($p < 0.05$). Complemented strains restored growth to near WT levels, indicating that the observed phenotypes were directly attributable to loss of *scrB* or *scrY* function.

2.4 | Loss of Function in *scrB* Alleles Encoded by *Pph* and *Psm* Highlights a Unique Role for Sucrose Metabolism in E-*Pae*

To identify potential reasons for the ineffective utilisation of sucrose by *Psm* R15244 or *Pph* 1448A, we focussed on the *scrB* gene given there were more nt/aa differences compared to *scrY*. The *scrB* allele from each strain was expressed in E-*Pae* 2250::*scrB* (E-*Pae*::*scrB*[pBBR1-$scrB_{Psm}$] and E-*Pae*::*scrB*[pBBR1-$scrB_{Pph}$]) and growth analysis in M9 + 50 mM sucrose was carried out. Neither gene was sufficient to restore full growth to the mutant compared to the WT E-*Pae scrB* allele (Figure 2E). Very little change in growth was observed using 10 mM sucrose (Figure S1E), whereas in 50 mM sucrose E-*Pae*::*scrB*[pBBR1-$scrB_{Psm}$] showed gradual increases reaching close to 0.4 OD towards the end (Figure 2E). E-*Pae*::*scrB*[pBBR1-$scrB_{Pph}$] did not exhibit any growth increase (Figure 2E). Statistical analysis confirmed these findings (Figure S2E): two-way repeated measures ANOVA showed significant effects of strain, time

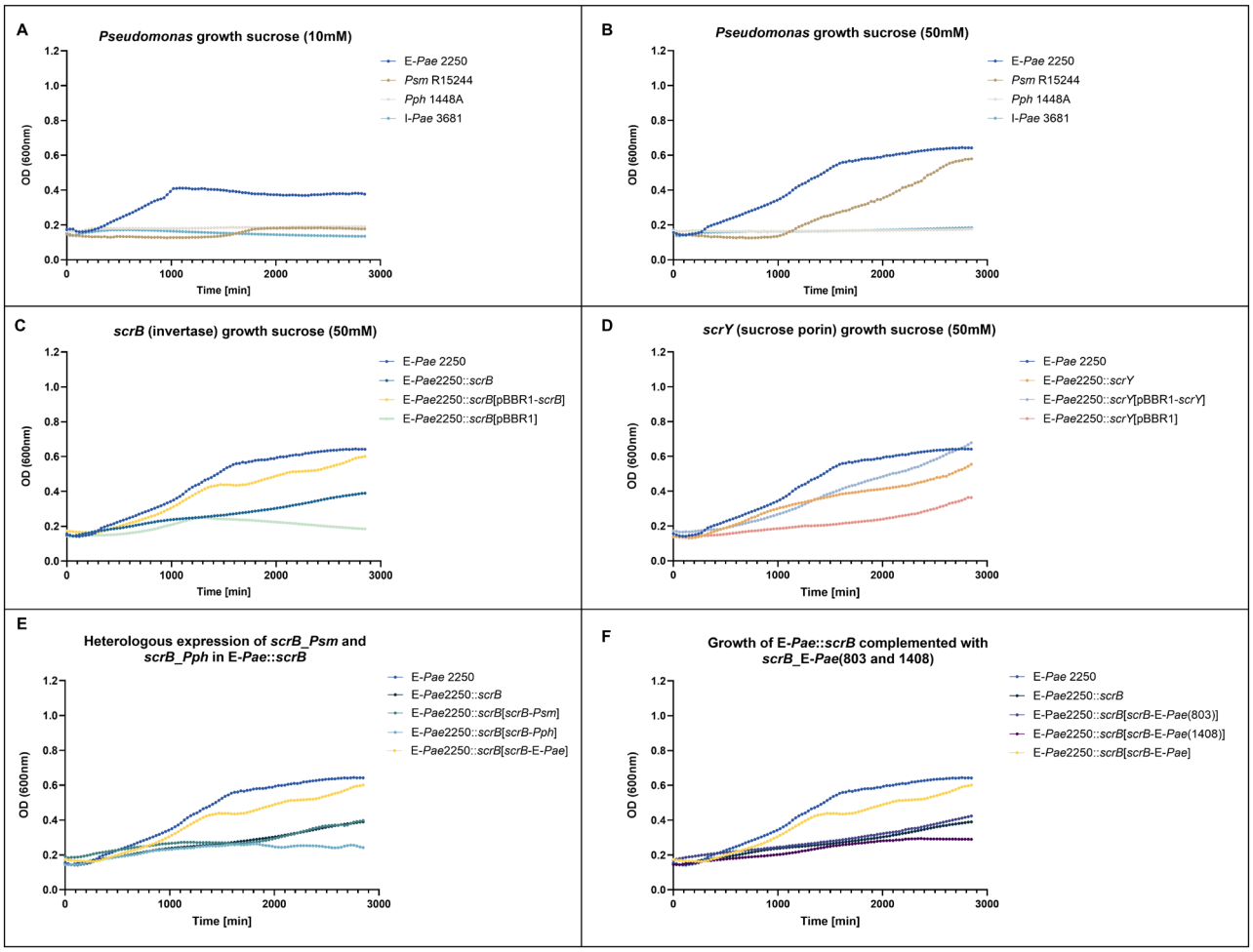

FIGURE 2 | Growth comparison of *Pseudomonas syringae* pv. *aesculi* (E-*Pae* 2250) and mutant strains on sucrose medium. (A, B) Growth of *Pseudomonas* wild-type strains in M9 minimal medium supplemented with sucrose at 10 and 50 mM, respectively. (C, D) Growth of E-*Pae*2250 *scrB* (invertase) and *scrY* (sucrose porin) knockout mutants in 50 mM sucrose-supplemented medium, respectively. (E) Functional complementation of E-*Pae*2250::*scrB* knockout mutant with heterologous *scrB* alleles from *P. syringae* pv. *morsprunorum* (*Psm*) R15244 and *P. syringae* pv. *phaseolicola* (*Pph*) 1448A. (F) Functional complementation of E-*Pae*2250::*scrB* knockout mutant with site-directed mutations introduced at the 803 and 1408 bp positions in the native *scrB* gene. All growth curves represent data from individual growth assays. While experiments were repeated independently with comparable trends, the data shown are from a single representative experiment. Optical density (OD_{600}) was measured at regular 30-min interval, and error bars represent standard deviation from technical triplicates. A more detailed statistical analysis is provided in Figure S2.

and interaction ($p < 0.001$), and post hoc Tukey–Kramer's tests indicated that neither heterologous strain showed a statistically significant improvement over the knockout at any time point ($p > 0.05$), highlighting a failure to complement. Notably, E-*Pae*::*scrB*[pBBR1-$scrB_{Psm}$] showed a gradual increase in growth by 3000 min, reaching $OD_{600} \sim 0.4$, but this was still significantly below WT levels ($p < 0.001$), while E-*Pae*::*scrB*[pBBR1-$scrB_{Pph}$] exhibited no measurable increase in OD.

These observations suggest that the lack of *Pph* growth is due to multiple mutations in $scrB_{Pph}$, whereas *Psm* is experiencing degradation of function due to one or more of the three aa changes (nt 97, 803 and 1408 corresponding to residues 97, 268 and 470). InterProScan analysis of ScrB revealed residue 268 is located in the N-terminal glycosylhydrolase domain, while residue 470 is found in the C-terminal glycosylhydrolase domain (Figure 1B). To examine this, site-directed mutagenesis of $scrB_{Pae}$ nucleotides to change residues 97 (A–G), 268 (G–A) and 470 (C–A) was attempted, but only mutations in 268 and 470 were achieved (Figure 1B). Both mutations led to reduced growth in M9 + 50 mM sucrose (Figure 2F), supported by statistical analysis (Figure S2F): the *scrB*-803 mutant (residue 268) was significantly impaired at all timepoints ($p < 0.001$), while the *scrB*-1408 mutant (residue 470) was only significantly different from WT at 1000 min ($p < 0.05$), with no significant difference from the *scrB* knockout at early timepoints ($p > 0.05$). These findings indicate both mutations impair ScrB function, with residue 268 likely being more critical. Neither mutant supported growth above $OD_{600} = 0.2$ in 10 mM sucrose (Figure S1F), underscoring the importance of these residues for optimal sucrose metabolism.

2.5 | The *Scr* Genes Are Important for *Pae* Virulence in Plants

The role of *scrB* and *scrY* in supporting E-*Pae* colonisation of plants and causing disease symptoms was investigated by

TABLE 2 | Alignment-based comparison of sucrose gene clusters in *Pseudmonas syringae* pv. *aesculi* (E-*Pae*), *P. syringae* pv. *morsprunorum* (*Psm*) and *P. syringae* pv. *phaseolicola* (*Pph*) strains, showing sequence differences and annotations.

Gene name	Strain	Minimum	Maximum	Length	Direction	# Differences to E-*Pae* 2250
LacI family DNA-binding transcriptional regulator	E-*Pae* 2250	7608	8600	993	Forward	—
cytR	*Psm* R14255	7608	8600	993	Forward	0
Transcriptional regulator	*Pph* 1448A	7595	8587	993	Forward	5
Glycoside hydrolase family 32 protein (*scrB*)	E-*Pae* 2250	6026	7540	1515	Forward	—
sacA	*Psm* R14255	6026	7540	1515	Forward	**5**
scrB	*Pph* 1448A	6013	7527	1515	Forward	94
Glycerol-3-phosphate ABC transporter	E-*Pae* 2250	4887	6029	1143	Forward	—
malK	*Psm* R14255	4887	6029	1143	Forward	4
malK	*Pph* 1448A	4874	6016	1143	Forward	44
Carbohydrate ABC transporter permease	E-*Pae* 2250	4014	4856	843	Forward	—
sugB	*Psm* R14255	4014	4856	843	Forward	3
Sugar ABC transporter	*Pph* 1448A	4001	4843	843	Forward	83
Sugar ABC transporter permease	E-*Pae* 2250	3055	4017	963	Forward	—
sugA	*Psm* R14255	3055	4017	963	Forward	1
Sugar ABC transporter	*Pph* 1448A	3042	4004	963	Forward	100
ABC transporter substrate-binding protein	E-*Pae* 2250	1759	3033	1275	Forward	—
CDS	*Psm* R14255	1759	3033	1275	Forward	9
Sugar ABC transporter	*Pph* 1448A	1746	3020	1275	Forward	109
Carbohydrate porin (*scrY*)	E-*Pae* 2250	14	1690	1677	Reverse	—
scrY	*Psm* R14255	14	1690	1677	Reverse	**9**
scrY	*Pph* 1448A	1	1677	1677	Reverse	43

Note: The bold values highlight the minimum nucleotide differences observed for the two genes that are the primary focus of this study. These genes were selected for detailed functional analysis throughout the paper.

inoculating the mutant and complemented mutant strains in its host (HC). The creation of E-*Pae* 2250 *hopAB1* and *hrpL* inactivation mutants served as useful controls as *hrpL* is a critical regulator and *hopAB1* was previously observed to be essential for full virulence/pathogenicity in HC.

E-*Pae* 2250 and *scrB*, *scrY*, *hopAB1* and *hrpL* mutant strains (and complemented strains) were inoculated into detached HC shoots. Disease assessment and pathogen growth analyses were conducted at 1, 3, 4 and 5 weeks post-inoculation (pi). The E-*Pae* 2250 caused typical disease symptoms on HC shoots characterised by rust-coloured liquid oozing on the branch, with necrotic phloem underlying the outer bark (Figure 3). No disease symptoms were observed for the *scrB*, *scrY*, *hopAB1* and *hrpL* knockout mutants (Figure 3), while the complemented strains displayed severe necrotic lesions similar to those observed in the WT strain (Figure 3A). The *scrB* and *scrY* knockout mutants had low disease scores on HC shoots comparable to the *hopAB1* and *hrpL* knockout mutants. Bacterial growth analysis in the plant showed that E-*Pae* 2250::*hrpL* and E-*Pae* 2250::*hopAB1* knockout mutants were significantly impaired in growth compared to E-*Pae* 2250 strain (Figure 4). In contrast, the growth of the E-*Pae* 2250::*scrY* and E-*Pae* 2250::*scrB* knockout mutants did not show a significant reduction compared to E-*Pae* 2250 (Figure 4). Consistently, bacterial growth in planta was significantly affected by strain type and timepoint (Figure S3). A two-way repeated measures ANOVA showed significant effects of strain ($p < 0.0001$), time ($p < 0.0001$) and their interaction ($p < 0.0001$), confirming distinct colonisation dynamics across strains. Tukey–Kramer post hoc tests showed that *scrB* and *scrY* mutants had significantly lower bacterial populations than E-*Pae* 2250 at multiple timepoints (Weeks 3–5), similar to the *hopAB1* and *hrpL* mutants. Complementation restored growth to E-*Pae* 2250 levels, confirming the importance of these genes in colonisation of woody tissue.

FIGURE 3 | Disease progression of *Pseudomonas syringae* pv. *aesculi* (E-*Pae* 2250), knockout mutants, and complemented strains on horse chestnut shoots. Symptoms were recorded at 1, 3, 4 and 5 weeks post-inoculation (10^8 CFU mL^{-1}) for E-*Pae* 2250, *scrB*, *scrY*, *hrpL* and *hopAB1* mutants, complemented strains and empty vectors. Columns show timepoints and rows correspond to bacterial strains. Symptoms included necrosis, tissue discolouration, and lesion development. This experiment was performed once with five biological replicates per strain, with each replicate corresponding to a different shoot.

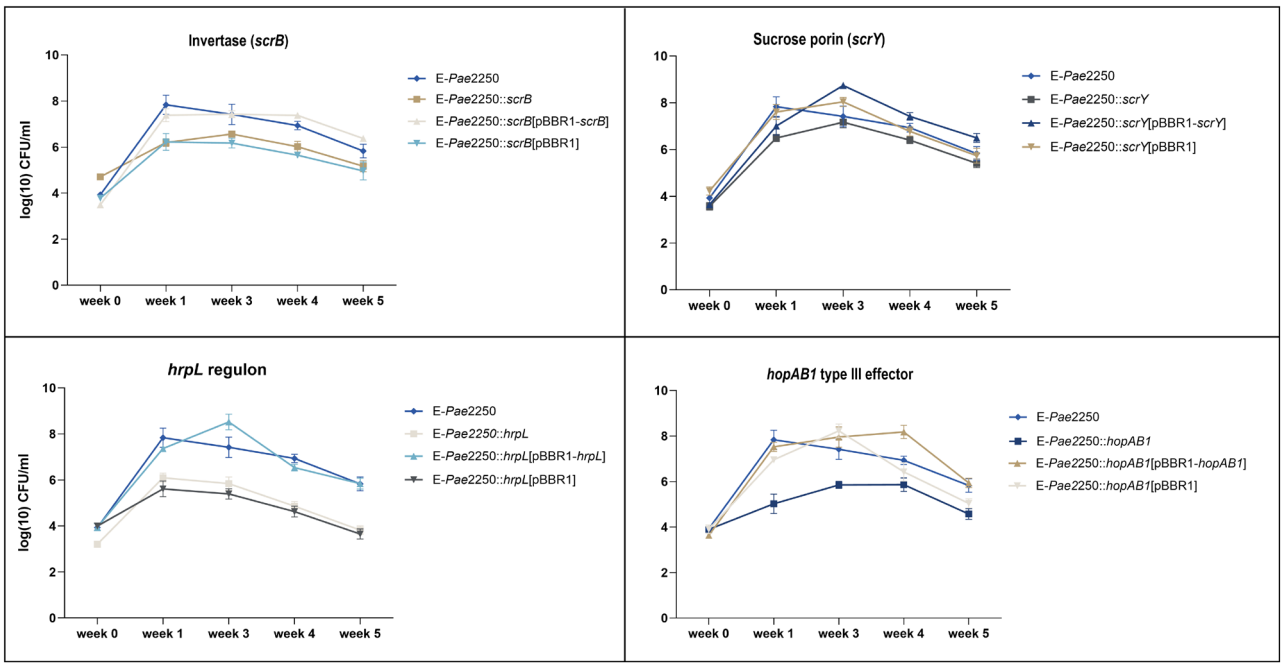

FIGURE 4 | Bacterial growth dynamics of *Pseudomonas syringae* pv. *aesculi* (E-*Pae* 2250), knockout mutants, and complemented strains over 5 weeks on horse chestnut shoots. Shoot inoculations were performed with 10^8 CFU mL^{-1} bacterial suspensions. Samples were taken at weekly intervals for 5 weeks. Bacterial populations (CFU mL^{-1}) were plotted over time, each data point represents the mean of five biological replicates; and error bars indicate the standard error of the mean (SEM). A more detailed statistical analysis is provided in Figure S3.

Although E-*Pae* is associated with diseased woody tissue, we also tested the various strains in HC leaves. Interestingly, strong necrotic symptoms appeared on HC leaves inoculated with E-*Pae* 2250 2 days post-inoculation (dpi), suggesting that E-*Pae* 2250 can cause disease symptoms in leaves at high inoculum levels (Figure 5). This was confirmed by in planta growth analysis (Figure 6).

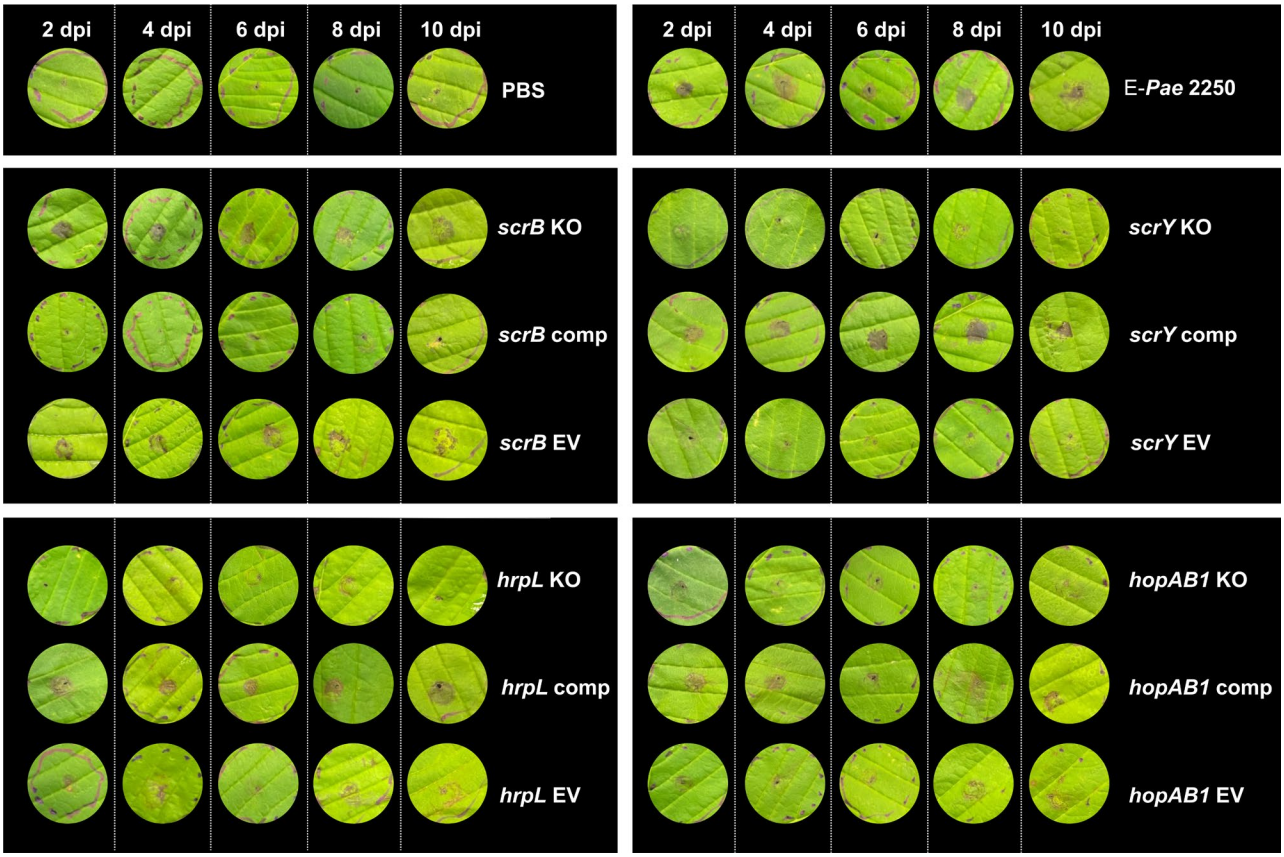

FIGURE 5 | Pathogenicity of *Pseudomonas syringae* pv. *aesculi* (E-*Pae* 2250) mutant strains on horse chestnut leaves. Leaves inoculated (10^8 CFU mL^{-1}) with E-*Pae* 2250, *scrY*, *hrpL*, *hopAB1* and *scrB* mutants, complemented strains, empty vectors and phosphate-buffered saline (PBS) control. Symptoms were assessed every 2 days after inoculation, for up to 10 days. E-*Pae* 2250 caused strong necrotic symptoms that were absent in PBS controls. Mutants *scrY*, *hrpL* and *hopAB1* did not cause necrosis, but complementation restored symptoms similar to E-*Pae* 2250. The *scrB* mutant induced necrosis similar to E-*Pae* 2250. Photos are representative of three independent biological replicates per treatment, with each strain inoculated on three separate leaves.

Inoculation with the mutants and complemented strains showed that the *scrY* (porin), *hrpL* and *hopAB1* mutants did not cause the same necrosis phenotype as WT, but that this could be recovered by complementation with their respective genes (Figure 5). Curiously, the *scrB* (invertase) mutant exhibited strong necrosis symptoms. Bacterial growth analysis showed the populations of the E-*Pae* 2250::*hrpL* and E-*Pae* 2250::*hopAB1* knockout mutants were significantly lower than that of E-*Pae* 2250 and complementation restored their growth to E-*Pae* 2250 levels (Figure 6). In contrast, the growth of the E-*Pae* 2250::*scrY* and *Pae* 2250::*scrB* knockout mutants mirrored the observations seen in woody tissue and did not show a significant reduction in growth compared to E-*Pae* 2250 (Figure 6). Growth analysis in leaves confirmed these findings (Figure S4). Two-way ANOVA indicated significant effects of strain and time ($p < 0.0001$), with one-way ANOVA and Tukey–Kramer's post hoc tests at 2 and 10 dpi further resolving strain-specific differences. At Day 2, *scrB*, *hrpL* and *hopAB1* complemented strains showed significantly increased populations relative to E-*Pae* 2250 ($p < 0.0001$), suggesting efficient colonisation. Meanwhile, the *scrB* mutant did not differ from WT ($p > 0.05$), in line with the observed necrosis, but *hrpL* and *hopAB1* mutants had significantly reduced populations ($p < 0.0001$). At Day 10, the *scrB* mutant remained statistically indistinguishable from E-*Pae* 2250 ($p > 0.05$), but the *scrY* mutant showed significantly reduced growth ($p < 0.0001$). Complementation of *scrB* showed an unexpected significant reduction in growth compared to E-*Pae* 2250 ($p < 0.0001$), while *hrpL* and *hopAB1* mutants still exhibited significantly lower populations ($p < 0.0001$). Their complemented strains remained slightly but significantly different from E-*Pae* 2250 ($p = 0.0444$), possibly reflecting variation in expression or vector-related effects.

3 | Discussion

Sucrose is abundant in plant tissues and can act both as a carbon source (Lemoine 2000) and as an osmolyte (Rolland et al. 2002). It is metabolised by many bacteria through enzymes like invertases and sucrose phosphorylases (Reid and Abratt 2005). Common features in sucrose-utilisation regulons include gene architecture, uptake systems and regulatory mechanisms. Reid and Abratt (2005) presented evidence of gene shuffling, with phylogenetic analyses suggesting that these gene clusters were acquired through horizontal gene transfer, facilitating bacterial colonisation of sucrose-rich niches. Our study focussed on the analysis of a seven-gene cluster in E-*Pae* that was predicted to be involved in sucrose utilisation. One gene encodes a putative LacI-family sucrose transcriptional regulator, another is predicted to be an invertase (ScrB) and the remaining five appear to be transporters, including a porin (ScrY).

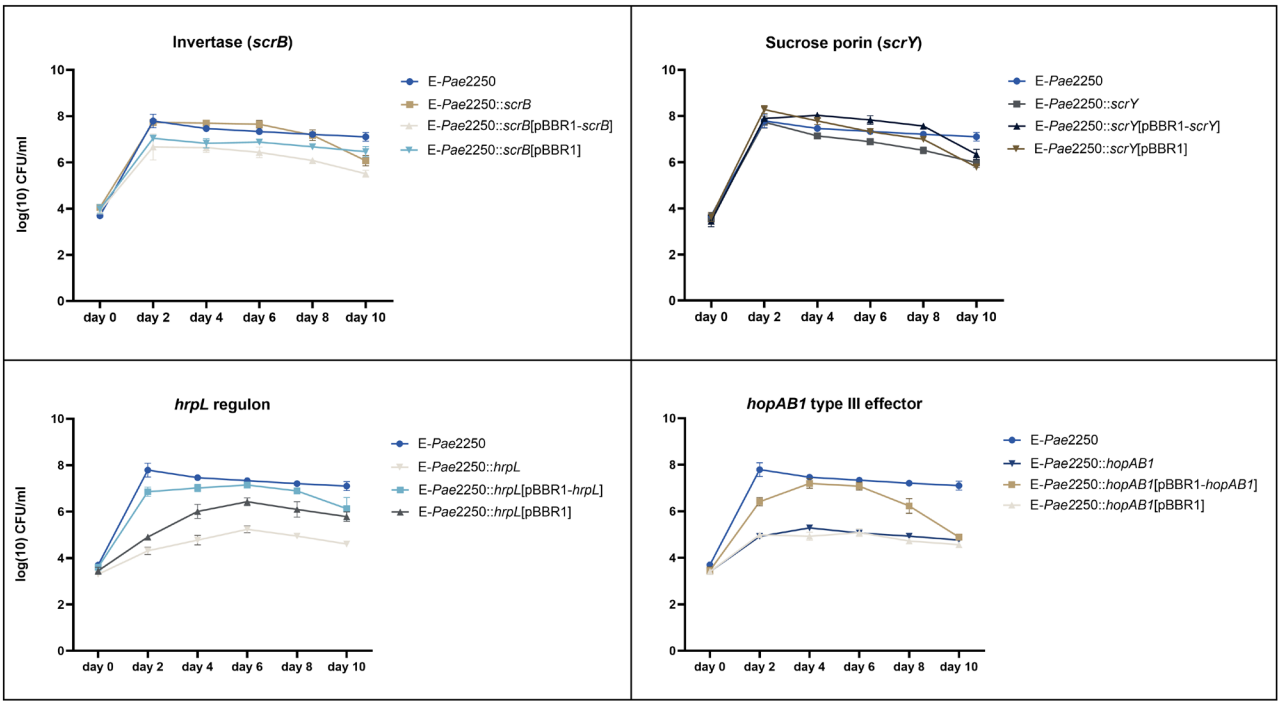

FIGURE 6 | Bacterial growth dynamics of *Pseudomonas syringae* pv. *aesculi* (E-*Pae* 2250), mutants and complemented strains on horse chestnut leaves over 10 days. Populations (CFU mL^{-1}) were plotted over time. Mutants *scrY*, *hrpL* and *hopAB1* showed reduced growth, while *scrB* growth was comparable to E-*Pae* 2250. Each data point represents the mean of three independent biological replicates, with error bars indicating the SEM. A more detailed statistical analysis is provided in Figure S4.

Our analysis of the *P. syringae* pangenome revealed that the sucrose gene cluster is present in 162 out of 206 strains, spanning diverse phylogroups, hosts and environments. We found that strains harbouring the *scr* gene cluster were significantly enriched in plant-pathogenic lifestyles, especially those infecting woody hosts and/or multiple tissues (leaf, fruit and stem). This association suggests that sucrose metabolism may provide a competitive advantage in complex plant tissues where nutrient availability and osmotic conditions fluctuate. Notably, 100% of strains isolated from woody hosts possessed the *scr* cluster, highlighting a potential role in adaptation to perennial plant environments, which are often more carbon-rich and osmotically variable. These findings reinforce the idea that the sucrose gene cluster contributes to pathogenesis and host colonisation, particularly in woody plants. However, the absence of the cluster in 44 strains suggests it is not essential for some lineages. Furthermore, variability in the nucleotide sequences of the sucrose cluster, particularly in *scrB* and *scrY*, suggests ongoing adaptation and possible degradation in certain strains. Thus, strains that colonise plants or environments with limited sucrose availability may not benefit from retaining this system, leading to its loss through genetic drift or negative selection.

E-*Pae* 2250 could efficiently metabolise sucrose, demonstrating robust growth in minimal medium supplemented with sucrose as the sole carbon source. In contrast, *Psm* R15244 and *Pph* 1448A showed limited or no growth under similar conditions, despite the presence of the sucrose gene cluster in their genomes. This disparity highlights potential differences in the functionality or regulation of the cluster among these strains. The lack of sucrose utilisation in I-*Pae* is consistent with the absence of the *scr* operon, though further testing, such as complementation, would be required to confirm a causal relationship. Mutational analysis of E-*Pae*'s *scrB* and *scrY* genes further confirmed their roles in sucrose metabolism, as inactivation of either gene significantly impaired growth on sucrose. Other studies have shown the importance of *scrB* and *scrY* in sucrose metabolism across various bacterial systems. For example, in *Escherichia coli*, a frameshift mutation in *scrY* reduced sucrose uptake under growth-limiting conditions (Hardesty et al. 1991). Similarly, deletion of *scrB* in *Clostridium beijerinckii* (Reid et al. 1999) and *Corynebacterium glutamicum* (Engels et al. 2008) abolished the ability to grow on sucrose. In *Erwinia amylovora*, deletion of *scrY* and *scrA* rendered the bacterium unable to utilise sucrose, highlighting the role of these genes in sucrose metabolism (Bogs and Geider 2000). However, further studies would be needed to determine their direct impact on pathogenicity. Collectively, these findings underscore the critical role of *scr* genes in sucrose metabolism and highlight the functional variability of the sucrose cluster among strains. The divergence observed in *Psm* and *Pph* may reflect evolutionary adaptations to specific ecological niches, where alternative metabolic pathways and carbon sources reduce the reliance on sucrose utilisation.

E-*Pae* is primarily known for causing bleeding canker on European HC trees (Green et al. 2009, 2010; Mcevoy et al. 2016; Steele et al. 2010; Webber et al. 2008), whereby it infects the vascular system of the tree, leading to characteristic bleeding lesions on the trunk. While E-*Pae* affects the trunk and branches, foliar infection of *Aesculus* species has also been reported under experimental conditions (Mullett and Webber 2013), demonstrating that leaves can serve as an additional site of infection. Our pathogenicity assays

confirmed that E-*Pae* is virulent in HC leaf and woody tissue. Necrotic and dark brown lesions developed in leaves within 48 h, along with tissue collapse. Pathogenicity assays on HC woody tissue consistently produced the characteristic symptoms of bleeding cankers, including dark, sticky exudates and discoloured, sunken lesions, similar to symptoms observed in natural infections. The *hopAB1* effector and *hrpL* alternative sigma factor are known to be critical pathogenicity factors for many *P. syringae* strains (Jackson et al. 1999), though *hopAB1* can also be recognised by some hosts to trigger immunity (Hulin et al. 2018). Inactivation of these genes in E-*Pae* showed they are essential to cause disease in HC, showing loss of symptoms and growth. Inactivation of the *scr* genes reduced E-*Pae* symptoms in leaves and wood. The *scrY* mutant showed minimal chlorosis and necrosis in HC leaves and failed to produce bleeding lesions in woody tissue. In contrast, the *scrB* mutant caused necrotic symptoms in leaves that were more severe than E-*Pae* 2250 but showed reduced symptoms in woody tissue. These findings highlight the importance of *scrB* and *scrY* for causing full virulence symptoms in woody tissue and *scrY* in leaves, but are not essential factors for growth, like *hopAB1* and *hrpL* (Figure S5). The observation that the *scrB* mutant displayed more severe symptoms in leaves might point to a niche-specific recognition of the pathogen via *scrB* in constraining full virulence symptoms. The reduced fitness observed in the *scrB* and *scrY* mutants on shoots, but not on leaves, suggests that these genes may be more critical for establishing infection in woody tissues. The enhanced disease symptoms of the *scrB* mutant in leaf tissue raise intriguing questions about the role of sucrose metabolism in different infection sites and reinforce recent observations that bacterial pathogens utilise distinct mechanisms to colonise different plant niches (Vadillo-Dieguez et al. 2024).

4 | Experimental Procedures

4.1 | Bacterial Strain, Plasmids and Growth Conditions

The bacterial strains and plasmids used in this study are described in Table 1. *P. syringae* strains were grown at 27°C in lysogeny broth (LB) (Bertani 1951) and King's medium B (KB) (King et al. 1954). *Escherichia coli* strains were grown in LB medium at 37°C. When required, the medium was supplemented with the following: gentamycin (Gm) (25 μg/mL), kanamycin (Km) (50 μg/mL) and ampicillin (Ap) (100 μg/mL). The pCR2.1 vector was used for the insertional mutagenesis experiments, containing a gene for kanamycin resistance. The broad-host-range plasmid pBBR1MCS-5 was used for complementation of the knockout mutants. For the sucrose utilisation assay, minimal medium (M9) (Stadtman 1957) was used, with sucrose as the sole carbon source.

4.2 | DNA Techniques for Mutagenesis and Analysis

Chromosomal DNA of E-*Pae* 2250 was isolated using a PureLink Genomic DNA Kit (Invitrogen) according to the manufacturer's instructions. The concentration and the purity of the genomic DNA were assessed using a NanoDrop 2000 spectrophotometer (ThermoFisher Scientific), with further quantification performed using a Qubit fluorometer (Invitrogen), for greater accuracy. PCRs were prepared using 2× Q5 high-fidelity master mix (NEB), with 10 μM forward primer, 10 μM reverse primer, 100 ng template DNA, and nuclease-free water. The primers used for gene deletion and complementation are listed in Table 2. The PCR amplification programme comprised denaturation at 98°C for 30; 35 cycles of 98°C for 10 s (denaturation step), 50°C–72°C (annealing, optimised using the NEB Tm Calculator) and 72°C for 20–30 s per kb (elongation step); and final elongation at 72°C for 2 min. After verifying the PCR product size by gel electrophoresis, the products were purified using either the Qiaquick PCR purification kit (Qiagen) or the Monarch Genomic DNA Purification Kit (NEB). Colony PCR, performed with 2× GoTaq Green Master Mix (Promega), was used to confirm the presence or absence of insert DNA in the plasmid constructs and knockout and complemented strains. The PCR conditions for this master mix included denaturation at 95°C for 5 min; 35 cycles of 95°C for 30 s (denaturation step), 50°C–72°C (annealing step) and 72°C for 1 min/kb (elongation step); and final elongation at 72°C for 5 min.

4.3 | Phylogenomic Analysis of *P. syringae* Sucrose-Gene Cluster

For the phylogenomic analysis of the *P. syringae* sucrose-gene cluster, a pangenome-based approach was used to infer phylogenetic relationships among 206 strains within the *P. syringae* species complex. Whole-genome data for these strains were retrieved from NCBI, and non-annotated genomes were processed using Prokka with default parameters (Seemann 2014). The annotated GFF files were then used as input for Panaroo, applying the strict stringency mode to identify core genes across isolates (Tonkin-Hill et al. 2020). Subsequently, IQ-TREE (Nguyen et al. 2015) was used to estimate maximum-likelihood phylogenies based on the core gene alignment obtained from Panaroo. The tree was constructed using ModelFinder to determine the best-fit substitution model, with 1000 ultrafast bootstrap replicates (-m MFP -b 1000 -alrt 100) to ensure robustness. The resulting tree was visualised using iTOL v. 6 (Letunic and Bork 2024), where multiple annotation features were applied to highlight the presence and absence of the sucrose-gene cluster across phylogroups. Our initial hypothesis was that the presence of the *scr* gene cluster might correlate with specific ecological or host associations, particularly among strains infecting woody hosts. To explore this, we annotated each strain in the dataset with metadata on isolation source, including host type (woody vs. non-woody), host tissue (leaf, stem, fruit) and environmental reservoirs (water, soil). These metadata are provided in Table S1,S6, and the species tree was correspondingly annotated in Figure 1C to indicate the presence or absence of the *scr* cluster alongside host type.

To assess the similarity of the sucrose gene cluster in E-*Pae* 2250 with other *Pseudomonas* strains, a MEGABLAST analysis was performed using the NCBI database, followed by multiple nucleotide and protein sequence alignments using MUSCLE (Geneious). Heatmaps and similarity matrices were

automatically generated to compare nucleotide sequence identities across different strains. The E-*Pae* sucrose gene cluster was used to search for homologous gene sequences across the pangenome using Blastn, with a minimum coverage threshold of 70% and an identity threshold of 80% to identify positive matches. For a strain to be classified as possessing the sucrose gene cluster, all seven genes were required to be present and located within a single genomic region, maintaining their predicted orientation and proximity (Figure 1A).

4.4 | Construction of Gene Knockout Vectors for E-*Pae* 2250

To construct *scrB*, *scrY*, *hopAB1* and *hrpL* mutants, an insertional inactivation strategy based on the principle of homologous recombination was used (Rozhdestvenskaya et al. 2010). All strains, vectors and plasmid constructs used in this study are detailed in Table 3. Knockout mutants of E-*Pae* 2250 were constructed as follows: for each knockout vector, two primers (Table 4) were designed to amplify most of the gene length using the whole genome sequence of E-*Pae* 2250. Two external restriction enzyme sequences matching multiple cloning sites of the pCR2.1 vector were also added to the primer sequences (Table 4). Prior to ligation, each of the insert DNA (amplified and purified as described above) and the vector were digested separately using the following recipe: 1 μg DNA, 10× compatible NEB buffer, 20 U each enzyme. The reaction mix was made to 50 μL with nuclease-free water and incubated for 1 h at 37°C. Products from the digest releasing a fragment at the expected size were purified with the Monarch PCR & DNA Cleanup Kit (NEB). The predigested and purified insert and vector were mixed and ligated with T4 ligase according to the following recipe: 100 ng vector, required mass insert (ng) for molar 3:1 ratio, 5× NEB ligase buffer, 5 U/μL T4 DNA ligase (NEB). The required mass insert was determined using the formula: required mass insert (ng) = desired insert/vector molar ratio × mass of vector (ng) × ratio of insert to vector lengths. The control reaction was prepared the same as the ligation reaction but with no insert DNA in the ligation mix. After incubation overnight at 4°C, the control and ligation reactions were purified using the Monarch PCR & DNA Cleanup Kit (NEB).

4.5 | Preparation of E-*Pae* 2250 Competent Cells

Pae electrocompetent cells were prepared following the protocol of Chuanchuen et al. (2002) developed for *Pseudomonas aeruginosa* and *E. coli* with minor modifications. Briefly, E-*Pae* 2250 cells were grown in 10 mL LB broth at 27°C overnight until they reached saturation ($OD_{600} = 1.5$). Aliquots of 1 mL of the stationary phase E-*Pae* culture were transferred to prechilled microcentrifuge tubes sitting on ice. Cells were then harvested at room temperature by centrifugation for 30 s at approximately 13,000 *g*. The cell pellets were resuspended with 750 μL of 0.5 M sterile ice-cold sucrose. The supernatant was removed and the cells were washed two more times with 750 mL of 0.5 M sterile ice-cold sucrose. The cell suspensions were kept on ice for 10 min and then centrifuged at approximately 13,000 *g* for 30 s at room temperature. After decanting the supernatant, the pellets were then resuspended in 200 μL 0.5 M sterile ice-cold sucrose and frozen until use.

4.6 | Transformation of Ligation Reaction

The purified controls and ligation reaction were transformed into *E. coli* DH5α, a strain compatible with blue and white screening, using chemically competent cells via heat-shock transformation following standard protocols (Sambrook and Maniatis 1990). After transformation, a 1:10 dilution of the reaction mixture was plated, and the remaining concentrated sample was spread onto LB Km plates containing Km (50 μg/mL) and 40 mg/mL X-gal (Merck). Plates were incubated overnight at 37°C. Three to five Km-resistant white colonies, indicating successful insertion, were selected from each transformation plate and grown overnight in LB broth supplemented with Km (50 μg/mL) at 37°C. Plasmid DNA was extracted from these cultures using the PureLink Quick Plasmid Miniprep Kit (Invitrogen). To verify the presence of the correct insert, 1 μg of plasmid DNA was subjected to restriction digestion in a 20 μL reaction volume containing 10 U of each of the appropriate restriction enzymes and a 10× NEB buffer compatible with both enzymes. The digested products were analysed by agarose gel electrophoresis to confirm the release of a fragment corresponding to the expected insert size. Candidate clones were sent for sequencing using M13F/R plasmid-specific primers (Table 4) to check for any point mutations in the insert.

4.7 | Transformation of E-*Pae* 2250 Cells by Electroporation

Recombinant plasmid DNA was used to electroporate into the cells of the WT strain E-*Pae* 2250. Electrocompetent cells of E-*Pae* 2250 were thawed on ice and 50 μL were aliquoted in sterile 1.5 mL tubes and suspended well by carefully flicking the tubes. For each gene knockout, 50 μg of recombinant plasmid DNA was added to electrocompetent cells, and the mix was placed on ice for 30 min. The transformation was then added to prechilled electroporation cuvettes (2 mm) (Bio-Rad). The electroporation of E-*Pae* 2250 was performed on a Gene Pulser (Bio-Rad) using the following parameters: capacitance 25 μFD, voltage 2.5 kV, resistance 400 Ω as adapted by Kámán-Tóth et al. (2018). Following electroporation, bacteria were suspended immediately with 1 mL KB medium and incubated at 27°C and 250 rpm for 4 h. The cells were then plated in a dilution series on KB supplemented with Km (50 μg/mL). Knockout mutants were then confirmed by PCR analysis using the conditions described for the GoTaq Green Master Mix (see above). This confirmation involved a combination of vector primers and gene-specific primers, as detailed in Table 4.

4.8 | Construction of Complemented Strains

To complement the knockout mutants, the WT gene of interest was reintroduced into the mutant strain on the broad-host range pBBR1MCS-5 (Table 3). Genes were PCR amplified using primers designed to amplify the full-length gene and to facilitate its ligation into the pBBR1MCS-5 vector (Table 4). The gene of interest was PCR amplified using primers designed to amplify the

TABLE 3 | Bacterial strains and plasmids used in this study.

Designation	Genotype	Relevant features	Source reference
E. coli			
DH5α	*Δ(argF-lac)169, φ80dlacZ58(M15), ΔphoA8, glnX44(AS), deoR481, rfbC1, gyrA96(Nal^R), recA1, endA1, thiE1 and hsdR17*	Str^R, Km^R, Ap^R	New England Biolabs
TOP10	F$^-$ *mcrA* Δ(*mrr-hsdRMS-mcrBC*) Φ80*lacZ*ΔM15 Δ*lacX74 recA1 araD139* Δ(*ara-leu*)7697 *galU galK rpsL endA1 nupG*	Sm^R, Str^R, Km^R, Ap^R	Invitrogen
S17-1 λpir	*thi pro hsdr$^-$ hsdM$^+$ recA* (chr::RP4 2-Tc::Mu- Km::Tn*7*)	RP4, Tp^R, Sp^R	Simon et al. (1983)
Pseudomonas syringae pathovars			
P. syringae pv. *aesculi* 2250 (E-*Pae* 2250)	Wild type	Nf^R, Ap^R	Isolated from horse chestnut in Pitlochry, UK (Green et al. 2010)
P. syringae pv. *aesculi* 6617 (E-*Pae* 6617)	Wild type	Nf^R, Ap^R	Isolated from horse chestnut in Pitlochry, UK (Green et al. 2010)
P. syringae pv. *aesculi* NCPPB-3681 (I-*Pae* 3681)	Wild type		Isolated from leaf-spot disease on Indian horse chestnut Durgapal and Singh (1980)
P. syringae pv. *phaseolicola* 1448A (*Pph* 1448A)	Wild type		Bean pathogen (Joardar et al. 2005)
P. syringae pv. *tabaci* 11528 (*Pta* 11528)	Wild type		Isolated from wild tobacco (Studholme et al. 2009)
P. syringae pv. *morsprunorum* R15244 (*Psm* R1-5244)	Wild type		Hulin et al. (2018)
E-*Pae* 2250 mutants			
E-*Pae* 2250::*scrB*	E-*Pae* 2250 knockout mutant for the *scrB* gene	Km^R	This study
E-*Pae* 2250::*scrY*	E-*Pae* 2250 knockout mutant for the *scrY* gene	Km^R	This study
E-*Pae* 2250::*hrpL*	E-*Pae* 2250 knockout mutant for the *hrpL* regulon	Km^R	This study
E-*Pae* 2250::*hopAB1*	E-*Pae*2250 knockout mutant for the *hopAB1* gene	Km^R	This study
E-*Pae* 2250::*scrB*[pBBR1-*scrB*]	E-*Pae* 2250::*scrB* complemented with pBBR1MCS-5 carrying the full length *scrB*	Gm^R	This study
E-*Pae* 2250::*scrY*[pBBR1-*scrY*]	E-*Pae* 2250::*scrY* complemented with pBBR1MCS-5 carrying the full length *scrY*	Gm^R	This study
E-*Pae* 2250::*hrpL*[pBBR1-*hrpL*]	E-*Pae* 2250::HrpL complemented with pBBR1MCS-5 carrying the full length *hrpL*	Gm^R	This study

(Continues)

TABLE 3 | (Continued)

Designation	Genotype	Relevant features	Source reference
E-*Pae* 2250::*hopAB1*[pBBR1-*hopAB1*]	E-*Pae* 2250::*hopAB1* complemented with pBBR1MCS-5 carrying the full length *HopAB1*	Gm^R	This study
E-*Pae* 2250::*scrB*[pBBR1]	E-*Pae* 2250::*scrB* carrying pBBR1MCS-5 empty vector	Km^RGm^R	This study
E-*Pae* 2250::*scrY*[pBBR1]	E-*Pae* 2250::*scrY* carrying pBBR1MCS-5 empty vector	Km^RGm^R	This study
E-*Pae* 2250::*hrpL*[pBBR1]	E-*Pae* 2250::*hrpL* carrying pBBR1MCS-5 empty vector	Km^RGm^R	This study
E-*Pae* 2250::*hopAB1*[pBBR1]	E-*Pae* 2250::*hopAB1* carrying pBBR1MCS-5 empty vector	Km^RGm^R	This study
E-*Pae* 2250::*scrB*[pBBR1-$scrB_{Psm}$]	E-*Pae* 2250 *scrB* knockout mutant carrying full fragment of *scrB* from *Psm* R15244 strain	Km^RGm^R	This study
E-*Pae* 2250::*scrB*[pBBR1-$scrB_{Pph}$]	E-*Pae* 2250 *scrB* knockout mutant carrying full fragment of *scrB* from *Pph* 1448A strain	Km^RGm^R	This study
E-*Pae* 2250::*scrB*[pBBR1-$scrB_{E\text{-}Pae2250(97)}$]	E-*Pae* 2250 *scrB* knockout mutant carrying full fragment of *scrB* from E-*Pae* 2250 carrying mutation at the 97 bp position	Km^RGm^R	This study
E-*Pae* 2250::*scrB*[pBBR1-$scrB_{E\text{-}Pae2250(803)}$]	E-*Pae* 2250 *scrB* knockout mutant carrying full fragment of *scrB* from E-*Pae* 2250 carrying mutation at the 803 bp position	Km^RGm^R	This study
E-*Pae* 2250::*scrB*[pBBR1-$scrB_{E\text{-}Pae2250(1408)}$]	E-*Pae* 2250 *scrB* knockout mutant carrying full fragment of *scrB* from E-*Pae* 2250 carrying mutation at the 1408 bp position	Km^RGm^R	This study
Plasmids and constructs			
pCR2.1-TOPO	TA PCR product cloning vector, ColE1 replicon, f1origin, lacZα, Ap^R, Km/Neo^R	Km^R	Invitrogen
pUC19	Cloning vector; *lacZ*α	Ap^R	Invitrogen
pBBR1MCS-5	$Gm\text{-}^R$, Tra^-, Mob^+, ungrouped replicon	Gm^R	Kovach et al. (1995)
pCR*scrB*-KO	pCR2.1 TOPO carrying 652 bp internal fragment of $scrB_{E\text{-}Pae2250}$	Km^R	This study
pCR*scrY*-KO	pCR2.1 TOPO carrying 589 bp internal fragment of $scrY_{E\text{-}Pae2250}$	Km^R	This study
pCR*hop*-KO	pCR2.1 TOPO carrying 900 bp internal fragment of $hopAB1_{E\text{-}Pae2250}$	Km^R	This study
pCR*hrp*-KO	pCR2.1 TOPO carrying 325 bp internal fragment of $hopAB1_{E\text{-}Pae2250}$	Km^R	This study

(Continues)

TABLE 3 | (Continued)

Designation	Genotype	Relevant features	Source reference
pBBR1*scrB*-comp	pBBR1MCS-5 carrying 1515 bp full fragment of $scrB_{E\text{-}Pae2250}$	Km^R Gm^R	This study
pBBR1*scrY*-comp	pBBR1MCS-5 carrying 1677 bp full fragment of $scrY_{E\text{-}Pae2250}$	Km^R Gm^R	This study
pBBR1*hop*-comp	pBBR1MCS-5 carrying 1626 bp full fragment of $HrpL_{E\text{-}Pae2250}$	Km^R Gm^R	This study
pBBR1*hrp*-comp	pBBR1MCS-5 carrying 555 bp full fragment of $hopAB1_{E\text{-}Pae2250}$	Km^R Gm^R	This study
pBBR1-$scrB_{Psm}$	pBBR1MCS-5 carrying 1515 bp full fragment of *scrB* from *Psm* R15244 strain	Gm^R	This study
pBBR1-$scrB_{Pph}$	pBBR1MCS-5 carrying 1515 bp full fragment of *scrB* from *Pph* 1448A strain	Gm^R	This study
pBBR1-$scrB_{Pae2250(97)}$	pBBR1MCS-5 carrying 1515 bp full fragment of *scrB* from E-*Pae* 2250 carrying mutation at the 97 bp position	Gm^R	This study
pBBR1-$scrB_{Pae2250(803)}$	pBBR1MCS-5 carrying 1515 bp full fragment of *scrB* from E-*Pae* 2250 carrying mutation at the 803 bp position	Gm^R	This study
pBBR1-$scrB_{Pae2250(1408)}$	pBBR1MCS-5 carrying 1515 bp full fragment of *scrB* from E-*Pae* 2250 carrying mutation at the 1408 bp position	Gm^R	This study

full-length gene and to facilitate its ligation into the pBBR1MCS-5 vector (Table 4). PCR conditions, ligation and transformation protocols followed those used for constructing the knockout vectors. To verify the correct plasmid construct, which should harbour the full-length gene, electrocompetent knockout mutant strains were prepared as described previously. Following electroporation of the plasmid into these strains, cells were plated on KB medium supplemented with gentamicin (Gm 25 μg/mL).

4.9 | Heterologous Expression and Site-Directed Mutagenesis

To assess the functional significance of mutations in the *scrB* gene on sucrose utilisation, we used both heterologous expression and site-directed mutagenesis (SDM) approaches. These targeted substitutions were based on alignment data with *Psm* R15244, which highlighted polymorphisms that could influence the protein's function (data not shown). For heterologous expression, we introduced *scrB* alleles from *Psm* R15244 and *Pph* 1448A into a *scrB* knockout mutant of E-*Pae* 2250 (E-*Pae* 2250::*scrB*) to generate the strains E-*Pae* 2250::*scrB*[pBBR1-$scrB_{Psm}$] and E-*Pae* 2250::*scrB*[pBBR1-$scrB_{Pph}$], respectively (Table 3). Complementation and SDM were performed using the broad-host-range plasmid pBBR1MCS-5 (Gm^R). Specific primers were designed to amplify the *scrB* gene from each strain (Table 4).

For SDM, specific nucleotide substitutions were introduced into the *scrB* gene at positions 803 and 1408, corresponding to amino acid changes at the active site, N-terminal and C-terminal regions, respectively. To introduce specific nucleotide substitutions in the *scrB* gene for SDM, primers were designed using the NEBaseChanger tool. For each mutation, the forward primer included the desired nucleotide change(s) at the centre, with at least 10 complementary nucleotides on the 3′ side of the mutation to ensure proper binding. The reverse primer was designed as the reverse complement of the region surrounding the mutation site, allowing the 5′ ends of the two primers to anneal back-to-back (Table 4). For SDM, we used the Q5 Site-Directed Mutagenesis Kit (New England BioLabs), where the kinase, ligase and DpnI (KLD) treatment was followed according to the manufacturer's instructions (New England BioLabs). This involved PCR amplification of the target gene with mutagenic primers, phosphorylation, ligation and DpnI digestion to degrade template DNA, facilitating the creation of the desired mutations within the *scrB* gene. After confirming the SDM plasmid constructs (pBBR1MCS-5) with single mutations, we introduced these plasmids into the *scrB* knockout mutant strain E-*Pae* 2250::*scrB*. This resulted in the generation of

TABLE 4 | Oligonucleotide primers and restriction enzymes used in this study.

Primer	Sequence (5′–3′)	Restriction enzyme site	Gene target
*scrB*KOF	GGTGGTGGATCCGCTTTTGATCCGTCAGGTGC	BamHI	*scrB* internal
*scrB*KOR	GGTGGTTCTAGACAGTTCGAGTTCGCGTGGC	XbaI	*scrB* internal
*scrB*compF	GGTGGTTCTAGAATGAGTTTTTCTGTGAATGC	XbaI	*scrB* full
*scrB*compR	GGTGGTGGATCCTCAATGATTTACCTGTAAGC	XbaI	*scrB* full
*scrY*KOF	GGTGGTGGATCCAGAAGCCTTCCCTGCCGAA	BamHI	*scrY* internal
*scrY*KOR	GGTGGTTCTAGACGCGGTGGGCCTTATACAA	XbaI	*scrY* internal
*scrY*compF	GGTGGTTCTAGACCAGGTTTCCATCTGGATGC	XbaI	*scrY* full
*scrY*compR	GGTGGTGGATCCAGTCCACATGCAGAACGC	BamHI	*scrY* full
*hrpL*KOF	GGTGGTGGATCCGCGCGTAATGAACCCGGA	BamHI	*hrpL* internal
*hrpL*KOR	GGTGGTTCTAGACATCTCCAGCGACACTTCC	XbaI	*hrpL* internal
*hrpL*compF	GGTGGTTCTAGAACCTAGTGATCCTTGATGC	XbaI	*hrpL* full
*hrpL*compR	GGTGGTGGATCCCGAACGGGTCAATCTGC	BamHI	*hrpL* full
*hopAB1*KOF	GGTGGTAAGCTTCTGCCTTCGAGATTGTACGC	HindIII	*hopAB1* internal
*hopAB1*KOR	GGTGGTGGATCCGACTGGAATCAGCAGCGAC	BamHI	*hopAB1* internal
*hopAB1*compF	GGTGGTGGATCCGGCGACCGATGCTCTCTTG	BamHI	*hopAB1* full
*hopAB1*compR	GGTGGTAAGCTTGTCCCGATTAGCGAACGAGG	HindIII	*hopAB1* full
Psm_{scrB}-Fwd	GTGGTGAGCTCAACACCTGACACACGAC	—	Forward primer for the *scrB* gene in *Pseudomonas syringae* pv. *morsprunorum* (Psm)
Psm_{scrB}-Rvs	GGTGGTCTCGAGCTGAGGTCATGCAAGGC	—	Full *scrB* gene in *Psm*
E-Pph_{scrB}-Fwd	GGTGGTGAGCTCAACACCTGACACACGAC	—	Full *scrB* gene in *P. syringae* pv. *phaseolicola* (Pph)
E-Pph_{scrB}-Rvs	GGTGGTCTCGAGCTGAGGTCATGCAAGGC	—	Full *scrB* gene in *Pph*
E-Pae_{scrB}-Fwd	GGTGGTGAGCTCAACACCTGACACACGAC	—	Full *scrB* gene in *P. syringae* pv. *aesculi* (E-*Pae)*
E-Pae_{scrB}-Rvs	GGTGGTCTCGAGCTGAGGTCATGCAAGGC	—	Full *scrB* gene in E-*Pae*
$scrB_{E\text{-}Pae}$-97_F	GGTAATCCACaatTATCGACCCG	—	Full *scrB* from E-*Pae* 2250 carrying mutation at the 97 bp position
$scrB_{E\text{-}Pae}$-97_R	TGCGCCAGGCTATCC	—	Full *scrB* from E-*Pae* 2250 carrying mutation at the 97 bp position
$scrB_{E\text{-}Pae}$-803_F	CCAAATCGACaacCAGTGGCAGT	—	Full *scrB* from E-*Pae* 2250 carrying mutation at the 803 bp position
$scrB_{E\text{-}Pae}$-803_R	CCCACTCGGTAGCCG	—	Full *scrB* from E-*Pae* 2250 carrying mutation at the 803 bp position
$scrB_{E\text{-}Pae}$--1408_F	CCTTTATCCAaagACCGACAGCC	—	Full *scrB* from E-*Pae* 2250 carrying mutation at the 1408 bp position
$scrB_{E\text{-}Pae}$--1408_R	CGACTACTGAAGCTGAAGC	—	Full *scrB* from E-*Pae* 2250 carrying mutation at the 1408 bp position
M13 rev (−29)	CAGGAAACAGCTATGAC	—	Universal primer
M13 uni (−21)	GTAAAACGACGGCCAGT	—	Universal primer
T3	AATTAACCCTCACTAAAGGG	—	Universal primer
T7	TAATACGACTCACTATAGGG	—	Universal primer

the strains E-*Pae* 2250::*scrB*[pBBR1-$scrB_{E\text{-}Pae2250(803)}$] and E-*Pae* 2250::*scrB*[pBBR1-$scrB_{E\text{-}Pae2250(1408)}$] (Table 3) each harbouring a specific nucleotide substitution at one of the targeted positions within the *scrB* gene. PCR amplification, ligation, transformation and electroporation into the E-*Pae* 2250::*scrB* knockout mutant followed the protocols described above. All generated strains, including those for heterologous expression and SDM, were assessed for sucrose utilisation as described above for other strains.

4.10 | Sucrose Assay

For the functional analysis of *scrB*, and *scrY* genes, WT, knockout mutants, complemented strains, and empty vectors controls were grown overnight in LB medium. Km (50 mg/mL) and/or Gm (25 mg/mL) were added to the medium when appropriate. After 24 h of incubation at 28°C supernatant, the bacterial cultures were centrifuged and the supernatant was removed. The cells were washed two to three times with M9 medium and resuspended in M9 minimal medium to an optical density (OD_{600}) of 0.2, corresponding to 2×10^8 CFU/mL. Growth experiments were conducted in liquid LB medium or liquid M9 minimal medium, supplemented with either 10 mM or 50 mM sucrose as carbon and energy sources. One hundred microlitres of bacterial culture and 100 μL of each medium were aliquoted into wells of a Greiner 96-well flat-bottomed plate (Thermo Fisher Scientific). Growth was monitored by measuring OD_{600} every 30 min for 48 h, with 10 s shaking period before each measurement, using the Tecan Spark Multimode Microplate Reader (Thermo Fisher Scientific). Each sample was replicated three times. To assess bacterial growth kinetics, doubling times were calculated using GraphPad Prism 10. Growth data were collected at regular intervals and plotted against time. The logarithm of the population was used as the y variable, and time was used as the x variable. Nonlinear regression was performed using the 'log of exponential growth' model from the growth equations panel in GraphPad Prism. This model fits the equation: $y=\log y_0+kx$, where $\log y_0$ is the starting population in logarithmic units and k is the rate constant. Doubling time (td) was calculated as $\ln_2/k$.

4.11 | Pathogenicity Assays

To study the implications of the *hopAB1*, *hrpL*, *scrB* and *ScrY* sucrose genes on E-*Pae* 2250 virulence, pathogenicity and colonisation, assays were performed on leaves and shoots of HC. Infection of detached HC leaves was followed using the protocol of Ruinelli et al. (2019). Leaves from wild European HC trees were freshly collected, surface-disinfected and air-dried under a sterile flow bench. Dormant 1-year-old HC shoots were collected and cut to approximately 15 cm in length. These were stored overnight in a cold, moist environment until inoculation. Five shoots per strain per time point were thoroughly disinfected with 70% ethanol for 5 min and allowed to air dry. For inoculation, bacteria were cultured overnight (18 h) on LB medium (supplemented with antibiotics when necessary) at 28°C with shaking at 200 rpm. The bacterial culture was then centrifuged at 3500 g for 5 min, and the resulting pellet was washed twice with sterile phosphate-buffered saline (PBS). The pellet was resuspended in sterile PBS and adjusted to an OD_{600} of 0.2, corresponding to approximately 10^8 CFU/mL. HC leaves were infiltrated with 50 μL of bacterial suspension using a 1 mL needle-less hypodermic syringe (Fisher Scientific), injecting into the intracellular spaces of the primary leaves. Sterile PBS was used as a negative control. Inoculated HC leaves were placed into self-sealed clear plastic boxes lined with Parafilm and incubated at 25°C for 1 week under daylight conditions. Symptoms on leaves were assessed and recorded every 2 days after inoculation and scored as follows: 0 = no symptom, 1 = yellowing, 2 = increased yellowing/chlorosis and 3 = strong tissue necrosis. A strain was considered pathogenic if it caused a clear brownish necrotic spot at the site of infiltration. For the HC shoot bioassay, inoculation was performed by making a cut wound and applying 50 μL of the bacterial suspension to the expanding leading shoot, approximately 1–2 cm above the previous year's terminal bud scar. The wounds were sealed with Parafilm, and the shoots were placed into sterile glass test tubes and incubated at 17°C for 5 weeks. Lesion development and disease severity were scored weekly based on observed lesion characteristics. Disease severity on inoculated HC shoots was scored on a scale from 0 to 5, where 0 = no symptoms, 1 = dry wood (no disease), 2 = browning liquid (onset of disease), 3 = necrotic lesion (intermediate lesion), 4 = browning and necrosis (advanced disease) and 5 = red oozing liquid (progressed and severe disease).

For pathogen fitness assessment, 7-mm leaf disks were cut from the infection area every 2 days after inoculation using Eppendorf snap caps. Four HC leaf disks were collected per strain. The disks were placed into 2 mL of sterile PBS and homogenised using a FastPrep Tissue Homogeniser (MP Biomedicals). Additionally, from inoculated HC shoots, a 1-cm section of shoot tissue was removed from the inoculated site, placed in 2 mL sterile PBS, and shaken for 1 h at 180 rpm at 27°C. Twenty microlitres of the homogenised leaf tissue and the shoot shake samples were diluted in 180 μL sterile PBS. Five microlitres of each of the 10^{-6}, 10^{-7} and 10^{-8} dilutions were plated onto selective media. Plates were incubated at 27°C, and CFU/mL were counted after 24–48 h. Data analysis was performed using GraphPad Prism v. 10.1.0 (www.graphpad.com).

Author Contributions

Sabrine Dhaouadi: conceptualization; investigation; formal analysis; data curation; methodology; visualization; writing – original draft; writing – review and editing; project administration. **Diana Vinchira-Villarraga:** methodology; investigation; formal analysis; writing – review and editing. **Sanju Bijarniya:** investigation; methodology; data curation; writing – review and editing. **Amy J. Webster:** formal analysis; methodology; writing – review and editing. **Federico Dorati:** methodology; investigation; writing – review and editing. **Carrie Brady:** resources; writing – review and editing. **Dawn L. Arnold:** supervision; writing – thorough review and editing. **Mojgan Rabiey:** supervision; validation; writing – review and editing; methodology. **Robert W. Jackson:** conceptualization; supervision; funding acquisition; resources; writing – original draft; writing – thorough review and editing; methodology; project administration. All work was carried out under the supervision of Robert W. Jackson.

Acknowledgements

We thank the JABBS Foundation for supporting Sabrine Dhaouadi, Diana Vinchira-Villarraga, Mojgan Rabiey and Robert W. Jackson. We also express our gratitude to Megan McDonald, Andy Plackett, Michelle

Hulin, Richard Harrison and John Mansfield for their helpful discussions and for sharing valuable protocols. Finally, we thank Stephen Hill for his horticultural expertise in managing the trees at the Wolfson Glasshouse facility.

Conflicts of Interest

The authors declare no conflicts of interest.

Data Availability Statement

The whole-genome sequence of *P. syringae* pv. *aesculi* is available in GenBank under the following accession numbers: BioProject PRJNA957756 and BioSample SAMN34263333. Whole-genome sequence (WGS) accessions, strain origins and all related data for the phylogenomic analysis are provided in Table S1.

References

Bertani, G. 1951. "Studies on Lysogenesis. I. The Mode of Phage Liberation by Lysogenic *Escherichia coli*." *Journal of Bacteriology* 62: 293–300.

Bogs, J., and K. Geider. 2000. "Molecular Analysis of Sucrose Metabolism of *Erwinia amylovora* and Influence on Bacterial Virulence." *Journal of Bacteriology* 182: 5351–5358.

Braun, D. M., L. Wang, and Y.-L. Ruan. 2013. "Understanding and Manipulating Sucrose Phloem Loading, Unloading, Metabolism, and Signalling to Enhance Crop Yield and Food Security." *Journal of Experimental Botany* 65: 1713–1735.

Bultreys, A., I. Gheysen, and V. Planchon. 2008. "Characterization of *Pseudomonas syringae* Strains Isolated From Diseased Horse-Chestnut Trees in Belgium." In *Pseudomonas syringae Pathovars and Related Pathogens – Identification, Epidemiology and Genomics*, edited by M. B. Fatmi, A. Collmer, N. S. Iacobellis, et al. Springer Netherlands.

Chuanchuen, R., C. T. Narasaki, and H. P. Schweizer. 2002. "Benchtop and Microcentrifuge Preparation of *Pseudomonas aeruginosa* Competent Cells." *BioTechniques* 33: 760–762.

de Keijzer, J., L. A. van den Broek, T. Ketelaar, and A. A. VAN Lammeren. 2012. "Histological Examination of Horse Chestnut Infection by *Pseudomonas syringae* pv. *aesculi* and Non-Destructive Heat Treatment to Stop Disease Progression." *PLoS One* 7: e39604.

Dijkshoorn-Dekker, M. W. C., and A. J. V. Kuik. 2005. Eindrapport Onderzoeksprogramma "Red de Kastanje voor Nederland."

Durgapal, J., and B. Singh. 1980. "Taxonomy of Pseudomonads Pathogenic to Horse-Chestnut, Wild Fig and Wild Cherry in India." *Indian Phytopathology* 33: 533–535.

Engels, V., T. Georgi, and V. F. Wendisch. 2008. "ScrB (Cg2927) is a Sucrose-6-Phosphate Hydrolase Essential for Sucrose Utilization by *Corynebacterium glutamicum*." *FEMS Microbiology Letters* 289: 80–89.

Green, S., B. Laue, C. G. Fossdal, S. W. A'hara, and J. E. Cottrell. 2009. "Infection of Horse Chestnut (*Aesculus hippocastanum*) by *Pseudomonas syringae* pv. *aesculi* and Its Detection by Quantitative Real-Time PCR." *Plant Pathology* 58: 731–744.

Green, S., D. J. Studholme, B. E. Laue, et al. 2010. "Comparative Genome Analysis Provides Insights Into the Evolution and Adaptation of *Pseudomonas syringae* pv. *aesculi* on *Aesculus hippocastanum*." *PLoS One* 5: e10224.

Gunasekaran, P., T. Karunakaran, B. Cami, A. G. Mukundan, L. Preziosi, and J. Baratti. 1990. "Cloning and Sequencing of the *sacA* Gene: Characterization of a Sucrase From *Zymomonas mobilis*." *Journal of Bacteriology* 172: 6727–6735.

Hardesty, C., C. Ferran, and J. M. Dirienzo. 1991. "Plasmid-Mediated Sucrose Metabolism in *Escherichia coli*: Characterization of *scrY*, the Structural Gene for a Phosphoenolpyruvate-Dependent Sucrose Phosphotransferase System Outer Membrane Porin." *Journal of Bacteriology* 173: 449–456.

Hulin, M. T., A. D. Armitage, J. G. Vicente, et al. 2018. "Comparative Genomics of *Pseudomonas syringae* Reveals Convergent Gene Gain and Loss Associated with Specialization onto Cherry (*Prunus avium*)." *New Phytologist* 219: 672–696.

Jackson, R. W., E. Athanassopoulos, G. Tsiamis, et al. 1999. "Identification of a Pathogenicity Island, Which Contains Genes for Virulence and Avirulence, on a Large Native Plasmid in the Bean Pathogen *Pseudomonas syringae* Pathovar *phaseolicola*." *Proceedings of the National Academy of Sciences of the United States of America* 96: 10875–10880.

Joardar, V., M. Lindeberg, R. W. Jackson, et al. 2005. "Whole-Genome Sequence Analysis of *Pseudomonas syringae* pv. *phaseolicola* 1448A Reveals Divergence among Pathovars in Genes Involved in Virulence and Transposition." *Journal of Bacteriology* 187: 6488–6498.

Kovach, M. E., P. H. Elzer, D. Steven Hill, et al. 1995. "Four New Derivatives of the Broad-Host-Range Cloning Vector pBBR1MCS, Carrying Different Antibiotic-Resistance Cassettes." *Gene* 166: 175–176.

Kámán-Tóth, E., M. Pogány, T. Dankó, Á. Szatmári, and Z. Bozsó. 2018. "A Simplified and Efficient *Agrobacterium tumefaciens* Electroporation Method." *3 Biotech* 8: 148.

King, E. O., M. K. Ward, and D. E. Raney. 1954. "Two Simple Media for the Demonstration of Pyocyanin and Fluorescin." *Journal of Laboratory and Clinical Medicine* 44: 301–307.

Lemoine, R. 2000. "Sucrose Transporters in Plants: Update on Function and Structure." *Biochimica et Biophysica Acta* 1465: 246–262.

Letunic, I., and P. Bork. 2024. "Interactive Tree of Life (iTOL) v6: Recent Updates to the Phylogenetic Tree Display and Annotation Tool." *Nucleic Acids Research* 52: W78–w82.

Mcevoy, A., F. O'regan, C. C. Fleming, et al. 2016. "Bleeding Canker of Horse Chestnut (*Aesculus hippocastanum*) in Ireland: Incidence, Severity and Characterization Using DNA Sequences and Real-Time PCR." *Plant Pathology* 65: 1419–1429.

Mertelik, J., K. Kloudova, I. Pankova, V. Krejzar, and V. Kudela. 2013. "Horse Chestnut Bleeding Canker Caused by *Pseudomonas syringae* pv. *aesculi* in The Czech Republic." *Acta Horticulturae* 990: 61–63.

Mullett, M. S., and J. F. Webber. 2013. "*Pseudomonas syringae* pv. aesculi: Foliar Infection of *Aesculus* Species and Temperature–Growth Relationships." *Forest Pathology* 43: 371–378.

Nguyen, L. T., H. A. Schmidt, A. VON Haeseler, and B. Q. Minh. 2015. "IQ-TREE: A Fast and Effective Stochastic Algorithm for Estimating Maximum-Likelihood Phylogenies." *Molecular Biology and Evolution* 32: 268–274.

Nowell, R. W., B. E. Laue, P. M. Sharp, and S. Green. 2016. "Comparative Genomics Reveals Genes Significantly Associated With Woody Hosts in the Plant Pathogen *Pseudomonas syringae*." *Molecular Plant Pathology* 17: 1409–1424.

Reid, S. J., and V. R. Abratt. 2005. "Sucrose Utilisation in Bacteria: Genetic Organisation and Regulation." *Applied Microbiology and Biotechnology* 67: 312–321.

Reid, S. J., M. S. Rafudeen, and N. G. Leat. 1999. "The Genes Controlling Sucrose Utilization in *Clostridium beijerinckii* NCIMB 8052 Constitute an Operon." *Microbiology* 145: 1461–1472.

Rolland, F., B. Moore, and J. Sheen. 2002. "Sugar Sensing and Signaling in Plants." *Plant Cell* 14, no. Suppl: S185–S205.

Rozhdestvenskaya, A. S., A. A. Totolian, and A. V. Dmitriev. 2010. "Inactivation of DNA-Binding Response Regulator Sak189 Abrogates β-Antigen Expression and Affects Virulence of *Streptococcus agalactiae*." *PLoS One* 5: e10212.

Ruinelli, M., J. Blom, T. H. M. Smits, and J. F. Pothier. 2019. "Comparative Genomics and Pathogenicity Potential of Members of the *Pseudomonas syringae* Species Complex on *Prunus* spp." *BMC Genomics* 20: 172.

Sambrook, J. F., and E. F. Maniatis. 1990. *Molecular Cloning, A Laboratory Manual*. 2nd ed. Spring Harbor. Cold Spring Harbor Laboratory Press.

Schmidt, O., D. Dujesiefken, H. Stobbe, U. Moreth, R. Kehr, and T. Schröder. 2008. "*Pseudomonas syringae* pv. *aesculi* Associated With Horse Chestnut Bleeding Canker in Germany." *Forest Pathology* 38: 124–128.

Seemann, T. 2014. "Prokka: Rapid Prokaryotic Genome Annotation." *Bioinformatics* 30: 2068–2069.

Simon, R., U. Priefer, and A. Pühler. 1983. "A Broad Host Range Mobilization System for In Vivo Genetic Engineering: Transposon Mutagenesis in Gram Negative Bacteria." *Bio/Technology* 1: 784–771.

Stadtman, E. 1957. "Preparation and Assay of Acyl Coenzyme A and Other Thiol Esters; Use of Hydroxylamine." *Methods in Enzymology* 3: 931–941.

Steele, H., B. Laue, G. Macaskill, S. Hendry, and S. Green. 2010. "Analysis of the Natural Infection of European Horse Chestnut (*Aesculus hippocastanum*) by *Pseudomonas syringae* pv. *aesculi*." *Plant Pathology* 59: 1005–1013.

Studholme, D. J., S. Ibanez, D. MacLean, J. L. Dangl, J. H. Chang, and J. P. Rathjen. 2009. "A Draft Genome Sequence and Functional Screen Reveals the Repertoire of Type III Secreted Proteins of *Pseudomonas syringae* Pathovar Tabaci 11528." *BMC Genomics* 10: 395.

Sun, L., F. Bertelshofer, G. Greiner, and R. A. Böckmann. 2016. "Characteristics of Sucrose Transport Through the Sucrose-Specific Porin ScrY Studied by Molecular Dynamics Simulations." *Frontiers in Bioengineering and Biotechnology* 4: 9.

Tauzin, A. S., and T. Giardina. 2014. "Sucrose and Invertases, a Part of the Plant Defense Response to the Biotic Stresses." *Frontiers in Plant Science* 5: 293.

Tonkin-Hill, G., N. MacAlasdair, C. Ruis, et al. 2020. "Producing Polished Prokaryotic Pangenomes with the Panaroo Pipeline." *Genome Biology* 21: 180.

Vadillo-Dieguez, A., Z. Zeng, J. W. Mansfield, et al. 2024. "Genetic Dissection of the Tissue-Specific Roles of Type III Effectors and Phytotoxins in the Pathogenicity of *Pseudomonas syringae* pv. syringae to Cherry." *Molecular Plant Pathology* 25: e13451.

Webber, J., N. Parkinson, J. Rose, H. Stanford, R. Cook, and J. Elphinstone. 2008. "Isolation and Identification of *Pseudomonas syringae* pv. *aesculi* Causing Bleeding Canker of Horse Chestnut in the UK." *Plant Pathology* 57: 368.

Supporting Information

Additional supporting information can be found online in the Supporting Information section.